V European Conference on Computational Fluid Dynamics
ECCOMAS CFD 2010
J. C. F. Pereira and A. Sequeira (Eds)
Lisbon, Portugal,14-17 June 2010

IMPLICIT PARTITIONED COUPLING WITH GLOBAL MULTIGRID IN FLUID-STRUCTURE INTERACTION

Stephen M. Sachs*, Dörte C. Sternel†, Michael Schäfer†

*Graduate School of Computational Engineering,
Technische Universität Darmstadt, Dolivostr. 15, 64293 Darmstadt
e-mail: sachs@gsc.tu-darmstadt.de
†Fachgebiet Numerische Berechnungsverfahren im Maschinenbau
Technische Universität Darmstadt, Dolivostr. 15, 64293 Darmstadt
e-mail: {sternel,schaefer}@fnb.tu-darmstadt.de

Key words: Geometric Multigrid Methods, Fluid-Structure Interaction, Arbitrary Lagrangian Eulerian Approach

Abstract. *In the simulation of fluid-structure interaction problems, a strong coupling of the solution processes for the underlying fluid and structure equations is as well desired as a high flexibility. In this work the implicit partitioned coupling approach is extended by applying the nonlinear geometric multigrid method globally to the coupled system. This moves the approach even closer to the strongly coupled, monolithic case and reduces computation time for the coupled algorithm without loss of flexibility. This implies the use of a geometric multigrid scheme in the structure solver in addition to the multigrid scheme in the flow solver.*

1 INTRODUCTION

Fluid-structure interaction (FSI) phenomena occur in many applications in industry and science. The numerical simulation of these phenomena is an ongoing challenge and several research groups are working on this topic. There are two main approaches to simulate FSI problems with well known advantages and drawbacks. On the one hand the numerically robust monolithic approach [6, 11] with its comparably low flexibility and on the other hand the highly adaptable but numerically challenging partitioned approach [14]. For the monolithic approaches, the entire coupled problem is solved simultaneously. The partitioned approach is based on coupling two separate codes for fluid and structure. The implicit partitioned coupling approach [16, 19] can be categorized as an approach in between partitioned and monolithic. Built from the partitioned approach it inherits its flexibility but gains more stability by several implicit coupling steps within one time step.

Subject of this contribution is the implementation of a global multigrid method in an existing implicit partitioned approach. The aim is to move even closer to the monolithic case and decrease computing time. Figure 2 illustrates the relation between the strength of the coupling, robustness, and adaptivity and a classification of different coupling approaches.

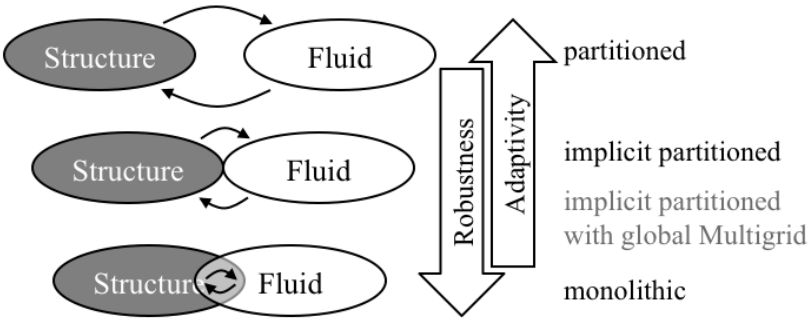

Figure 1: Coupling Approaches

In the implicit partitioned approach employed, the fluid system is simulated by the finite-volume solver FASTEST [7]. It uses the SIMPLE algorithm for pressure correction and the SIP [17] solver for the linearized systems. The structure is solved by the finite-element code FEAP [8] and coupling is realized by the MpCCI [12] coupling interface. The coupled system is assembled in an Arbitrary Lagrangian Eulerian (ALE) formulation.

While the use of a geometric multigrid method is a common way to accelerate the solution of flow solvers, this is not the case for structure solvers. Hence, in realizing the global multigrid approach, the first step is the implementation of a geometric multigrid into the structure solver. Afterwards, the coupling of fluid and structure on all grid levels is realized.

We first formulate the coupled system in the ALE framework and continue with the theory of the global multigrid approach and the implemented algorithms. A validation of the newly implemented geometric multigrid method in the structure solver is shown, as well as a comparison between the implicit partitioned approach and the implicit partitioned approach with global multigrid.

2 NUMERICAL METHODS

In this section the FSI system is formulated based on the conservation laws, the coupling conditions, and the material properties. Then this system is discretized in space and time.

2.1 Coupled FSI system in ALE Framework

In order to formulate the coupled FSI system we use the conservation equations in the ALE framework to assemble the Navier-Stokes equations for incompressible Newtonian fluids and the elasticity equation. As structural material model the St. Venant Kirchhoff constitutive relation is used. This can be easily exchanged by other models. Let Ω be our computational FSI domain, described in the ALE framework, which has a disjoint partition into the structure domain Ω_s and the fluid domain Ω_f with FSI boundary $\Gamma = \overline{\Omega}_s \cap \overline{\Omega}_f$. Let $\mathcal{V}$, $\mathcal{P}$, $\mathcal{U}$ be the appropriate function spaces with all boundary conditions on the remaining boundaries $\partial\Omega\backslash\Gamma$ embedded. Velocity, pressure, and displacement are denoted by $(v, p, u) \in \mathcal{V} \times \mathcal{P} \times \mathcal{U}$. The coupled problem can then be stated as

$$\frac{\partial}{\partial t}\int_\Omega \rho v \; dV + \int_{\partial\Omega} \rho(v - v^g) v n \; dA = \int_{\partial\Omega} \sigma n \; dA + \int_\Omega \rho f \; dV \quad \text{in } \Omega \tag{1}$$

$$\frac{\partial}{\partial t}\int_\Omega \rho \; dV + \int_{\partial\Omega} \rho(v - v^g) \; n \; dA = 0 \quad \text{in } \Omega_f \tag{2}$$

$$\sigma = \mu_f(\nabla v + \nabla v^T) - pI \text{ in } \Omega_f \tag{3}$$

$$\frac{\partial}{\partial t} u = v \quad \text{in } \Omega_s \tag{4}$$

$$\sigma = \lambda_s \; \mathrm{tr}(E) \; I + 2\mu_s E \text{ in } \Omega_s \tag{5}$$

$$E = \frac{1}{2}\left(\frac{\partial x}{\partial X}^T \frac{\partial x}{\partial X} - I\right) \tag{6}$$

$$\Delta u = 0 \quad \text{in } \Omega_f \tag{7}$$

$$\Delta p = 0 \quad \text{in } \Omega_s \tag{8}$$

with σ the Cauchy stress tensor, μ_f the dynamic viscosity, λ_s, and μ_s the Lamé constants and E The Green Lagrange strain tensor. The FSI boundary conditions for the fluid

$$v_f = v_s \quad \text{on } \Gamma \tag{9}$$

and for the structure

$$\sigma_s n_s = \sigma_f n_f \quad \text{on } \Gamma \tag{10}$$

are implicitly stated in the system (1)-(8), as v and σ are defined continuously on Ω. Note, that the FSI boundary conditions for the fluid computation are of Dirichlet type,

thus will be incorporated into the discretized system. The FSI boundary conditions on structure side are of von Neumann type, thus have to be treated separately.
The harmonic continuations of the pressure and displacement fields are needed for a global description within function spaces defined on Ω.
For the fluid part equations (1) and (3) reduce to

$$\frac{\partial}{\partial t}\int_\Omega \rho v \; dV + \int_{\partial\Omega} \rho(v - v^g) v n \; dA - \int_{\partial\Omega} \mu(\nabla v + \nabla v^T) n \; dA = -\int_{\partial\Omega} p n \; dA + \int_\Omega \rho f \; dV \;\text{ in } \Omega_f. \tag{11}$$

For the structure part, as $v = v^g$, the momentum equation (1) reduces to

$$\frac{\partial}{\partial t}\int_\Omega \rho v \; dV - \int_{\partial\Omega} \sigma n \; dA = \int_\Omega \rho f \; dV \text{ in } \Omega_s. \tag{12}$$

2.2 Space Conservation Law

The mass conservation equation in the ALE framework has to be fulfilled in every time step. In [3] it is shown, that this is a nontrivial task. In order to check this property the so called Space Conservation Law is introduced:

$$\frac{\partial}{\partial t}\int_\Omega \rho \; dV = \int_{\partial\Omega} \rho v^g \; n \; dA \;\text{ in } \Omega_f \tag{13}$$

which is (2) in the case of $v = 0$. The discrete counterpart of this equation is implemented but will not be further discussed here.
If the Space Conservation Law is fulfilled, (2) reduces to the same form as in the Eulerian case:

$$\int_{\partial\Omega} \rho v \; n \; dA = 0 \;, \text{ on } \Omega_f. \tag{14}$$

2.3 Spatial Discretization

In the following, the triple $(v, p, u) \in \mathcal{V} \times \mathcal{P} \times \mathcal{U}$ will be referred to as w. The Navier-Stokes equations (9), (11), and (14) are discretized using a fully conservative finite-volume approach. In order to improve stability, the convective and diffusive fluxes are divided into implicit parts $\bar{A}(w)$ and explicit parts which contribute to the source terms. Singly the upwind convection fluxes and normal diffusion fluxes are treated implicitly. The pressure term is discretized into a linear form $D(p)$ and the source terms into a nonlinear form $\bar{b}(w)$.
The assembled spatially discretized system then can be written as

$$\frac{\partial}{\partial t} v \rho \, \delta V + \bar{A}(w)v + D(w)p = \bar{b}(w) \tag{15}$$

$$B(w)v = 0 \tag{16}$$

with δV being the discrete volume of the current grid cell. Note that the convective flux of the ALE grid velocity appears in the implicitly treated parts in $\bar{A}(w)$ as well as the

explicitly treated parts in $\bar{b}(w)$. The Dirichlet boundary conditions (9) are already integrated into the system.

The elasticity equation (12) together with the stress and strain tensors (5), (6), and relationship (4) are discretized by a Galerkin finite-element approach. The resulting system is

$$M\frac{\partial}{\partial t}v + N(\sigma) = f \tag{17}$$

with M the mass matrix, $N(\sigma)$ the stress divergence vector, and f the sum of the body forces and the boundary loadings.

The FSI boundary condition on structure side (10) is realized by a linear operator C defined on the interface Γ:

$$f = C(p). \tag{18}$$

The grid movement in Ω_f is realized as proposed by [15].

2.4 Temporal Discretization

The unsteady term in (15) is discretized by a second-order accurate backward difference discretization. The discretization complies with the product rule, as proposed by [5].

$$\frac{\partial}{\partial t}v\rho\,\delta V \approx \frac{3v^{n+1} - 4v^n + v^{n-1}}{\Delta t}\rho\,\delta V^{n+1} + \frac{3\delta V^{n+1} - 4\delta V^n + \delta V^{n-1}}{\Delta t}\rho v^{n+1}. \tag{19}$$

Using the latter equation, the system (15) and (16) results in:

$$A(w)v + D(w)p = b(w) \tag{20}$$

$$B(w)v = 0. \tag{21}$$

The temporal discretization on structure side is realized by Newmarks beta method. Equation (17) then reads:

$$K\Delta u = R \tag{22}$$

$$u^{n+1} = u^n + \Delta u \tag{23}$$

$$v^{v+1} = v^n + \frac{\gamma}{\beta\Delta t}\Delta u \tag{24}$$

$$a^{n+1} = a^n + \frac{1}{\beta\Delta t^2}\Delta u \tag{25}$$

$$\text{with } R = f - M\frac{\partial}{\partial t}v - N(\sigma)\ ,\ K = -\left[\frac{\partial R}{\partial u} + \frac{\partial R}{\partial v}\frac{\partial v}{\partial u} + \frac{\partial R}{\partial a}\frac{\partial a}{\partial u}\right].$$

Finally, equations (22) to (25) yield the discrete second-order time accurate equation

$$K(w) = f(w). \tag{26}$$

3 MULTIGRID METHODS

Within this section the multigrid method is applied to the coupled problem. In the first part a short motivation of the nonlinear multigrid method or full approximation scheme (FAS) is given [2, 9]. Thereafter the coupled discrete FSI problem is solved by the FAS.

3.1 Full Approximation Scheme

A short motivation of the FAS is based on Newtons method. Considering the nonlinear system of equations

$$A(x) = b(x) \ , \ R(x) = b(x) - A(x) \tag{27}$$

with $R(x)$ the residual. Let the computational domain be discretized by m successive coarser grids g^l, $l = 1, \ldots, m$, and let x^l and R^l be the discretization of x and R on g^l. Newtons method claims (27) discretized on grid g^l can be solved by iterating

$$-\frac{\partial R^l(x_n^l)}{\partial x}\Delta x^l = R^l(x_n^l) \tag{28}$$

$$x_{n+1}^l = x_n^l + \Delta x^l \tag{29}$$

with n being the iteration number. Let $\tilde{x}^l$ be the current solution of the system (28), (29) and the starting point for the next equation. By restricting equation (28) to g^{l+1} the next step of Newtons method yields

$$-\frac{\partial R^{l+1}(x_n^{l+1})}{\partial x}\Delta x^{l+1} = I_l^{l+1} R^l(x_n^l) \tag{30}$$

$$x_{n+1}^l = x_n^l + \mathcal{I}_{l+1}^l \Delta x^{l+1} \tag{31}$$

with $\mathcal{I}_l^{l+1}$ being the interpolation operator from grid g^l to g^{l+1}. By approximating the gradient by finite difference this results in the coarse grid correction for the FAS:

$$A^{l+1}(x_{n+1}^{l+1}) = b^{l+1}(x_{n+1}^{l+1}) - b^{l+1}(\mathcal{I}_l^{l+1} x_n^l) + A^{l+1}(\mathcal{I}_l^{l+1} x_n^l) + \mathcal{I}_l^{l+1} R^l(\tilde{x}^l) \tag{32}$$

$$x_{n+1}^l = x_n^l + \mathcal{I}_{l+1}^l (x_{n+1}^{l+1} - \mathcal{I}_l^{l+1} x_n^l) \ . \tag{33}$$

Note, that the second and third right hand side terms of (32) are dependent on $\mathcal{I}_l^{l+1} x_n^l$. This value can not be updated during computation of (32), as this is just one single step in Newtons method. Application of this scheme to the coarse grid equation (32) will result in a correction on grid g^{l+2}. Thus, the multigrid scheme is a straightforward extension of the two grid scheme and for further discussion only the two grid scheme will be used.

3.2 Solution Algorithm

We recall the fully discretized nonlinear system for an unsteady coupled computation (18), (20), (21) and (26) discretized on grid size l:

$$A^l(w^l)v^l + D^l(w^l)p^l = b^l(w^l) \tag{34}$$

$$B^l(w^l)v^l = 0 \tag{35}$$
$$f^l = C^l(p^l) \tag{36}$$
$$K^l(w^l) = f^l(w^l)\,. \tag{37}$$

This system has to be solved globally by the FAS embedding custom solvers locally for each subproblem: Equations (34) and (35) are solved using the flow solver FASTEST. (34) is linearized by fix point iteration, (35) is used as the pressure correction in the SIMPLE algorithm, and the resulting linear problems are solved by the SIP. Equation (36) is solved in the flow solver and the discrete loading values are interpolated in the coupling interface MpCCI. Equation (37) is solved in the structure solver FEAP. It is linearized by Newtons method and the resulting linear systems are solved by the Gauß-Seidel method.
The restriction in the fluid domain is done by linear interpolation of 8 adjacent grid cells, in the structure domain it is defined similar to the Galerkin approach. As stated in [9], linear interpolation operators are sufficient to solve second-order pdes.
After a few fine grid iterations (pre-smoothing) the entire system is restricted to the next coarser grid level:

$$\begin{aligned} A^{l+1}(w^{l+1})v^{l+1} + D^{l+1}(w^{l+1})p^{l+1} &= b^{l+1}(w^{l+1}) - b^{l+1}(\mathcal{I}_l^{l+1}\tilde{w}^l) \\ &\quad + A^{l+1}(\mathcal{I}_l^{l+1}\tilde{w}^l)\mathcal{I}_l^{l+1}\tilde{v}^l + D^{l+1}(\mathcal{I}_l^{l+1}\tilde{w}^l)\mathcal{I}_l^{l+1}\tilde{p}^l \\ &\quad + \mathcal{I}_l^{l+1}\left[b^l(\tilde{w}^l) - A^l(\tilde{w}^l)\tilde{v}^l - D^l(\tilde{w}^l)\tilde{p}^l\right] \end{aligned} \tag{38}$$
$$B^{l+1}(w^{l+1})v^{l+1} = B^{l+1}(\mathcal{I}_l^{l+1}\tilde{w}^l)\mathcal{I}_l^{l+1}\tilde{v}^l - \mathcal{I}_l^{l+1}\left[B^l(\tilde{w}^l)\tilde{v}^l\right] \tag{39}$$
$$\begin{aligned} K^{l+1}(w^{l+1}) &= f^{l+1}(w^{l+1}) - f^{l+1}(\mathcal{I}_l^{l+1}\tilde{w}^l) + K^{l+1}(\mathcal{I}_l^{l+1}\tilde{w}^l) \\ &\quad + \mathcal{I}_l^{l+1}\left[f^l(\tilde{w}^l) - K^l(\tilde{w}^l)\right]\,. \end{aligned} \tag{40}$$

with $\tilde{w}^l$ the current fine grid solution.
Note, that for the linear relation (36) FAS reduces to the same relation discretized on a coarser grid. This is one of the advantages of the FAS, because the same routines can be used for several discretizations.

As the restricted mass conservation equation (39) is based on fluxes defined on the fine grid, and therefore on the fine grid geometry, the coarse grid velocities do not necessarily have to fulfill this equation. Therefore the coarse grid fluxes used in this equation are not calculated from the restricted velocities, but from mass fluxes, which are restricted too.
Let $\tilde{w}^{l+1}$ be the current coarse grid solution after coarse grid correction. Then the current fine grid solution can be corrected as:

$$w^l = \tilde{w}^l + \mathcal{I}_{l+1}^l\left(w^{l+1} - \mathcal{I}_l^{l+1}\tilde{w}^l\right). \tag{41}$$

After correction another few fine grid iterations (post-smoothing) are needed in order to eliminate high-frequency errors that arise from the interpolation.

4 TEST CASE I

In this section a 2D structure problem is calculated, in order to verify the implementation of the FAS in the structure solver. As it was shown in earlier work, that the multigrid coupling with an FAS on fluid side and a single grid computation on structure side generates a significant speedup [10], singly the geometric multigrid method on structure side is verified here.

4.1 Problem Description

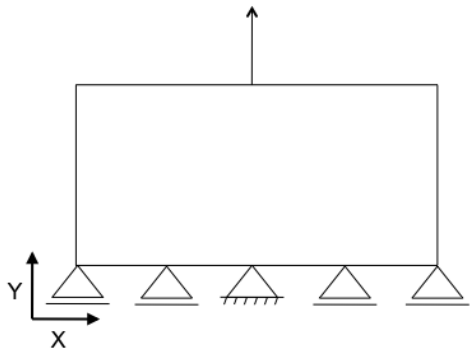

Figure 2: 2D Point load

The problem setup is a rectangular body with an applied point load. The computational domain is a 2×1 [m^2] rectangle. Boundary conditions are: Fixed in y direction at the bottom, clamped at the bottom center node, and a point load is applied to the top center node. The remaining boundaries have zero loading. The domain is discretized by 5 successively coarsened grids from 16,770 to 90 degrees of freedom. Linear elastic material is used and a steady state solution is computed. This test case is based on the problem description in [13].

4.2 Results

Two setups are investigated. The first setup **Two Grid** uses a two-grid scheme on all 4 grid levels. The second setup **Max Grid** always uses the maximum number of available grids. As a smoother the Gauß-Seidel method has been implemented into the structure solver FEAP, the system on the coarsest grid is solved by a LAPACK [1] direct solver. The convergence criterion is $\frac{||R||_2}{||f||_2} < 10^{-6}$, with R the residual and f the applied load.

Setup	$n = 306$	$n = 1,122$	$n = 4,290$	$n = 16,770$
Max Grid	4.9	5.0	4.2	3.7
Two Grid	4.9	5.1	5.1	5.1

Table 1: No. of multigrid cycles to convergence

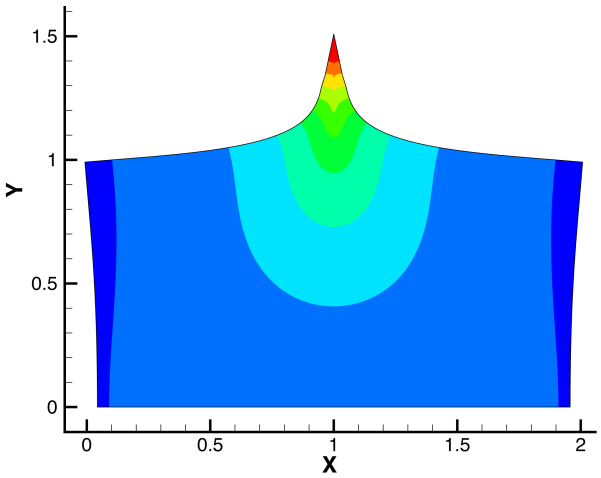

Figure 3: y-Displacement on grid 1: 16.770 DOFs

Table 1 shows the number of multigrid cycles needed for the system to converge. The values are not integer, as linear interpolation of the convergence criterion is used. The **Max Grid** setup shows a decrease in multigrid cycles needed, which will eventually approach a constant value. The **Two Grid** scheme shows constant behavior. This shows the independence of the number of multigrid cycles of the size of the underlying discretization.

5 TEST CASE II

In this section the global multigrid coupling approach is applied to a 3D FSI test case. The geometry is taken from the FSI Benchmark [18]. The test case consists of a channel flow around a rigid cylinder with an elastic bar attached to it. The computational cost of the new approach is compared to the implicit partitioned coupling approach by the number of fine grid iterations used by the flow solver.

5.1 Problem Description

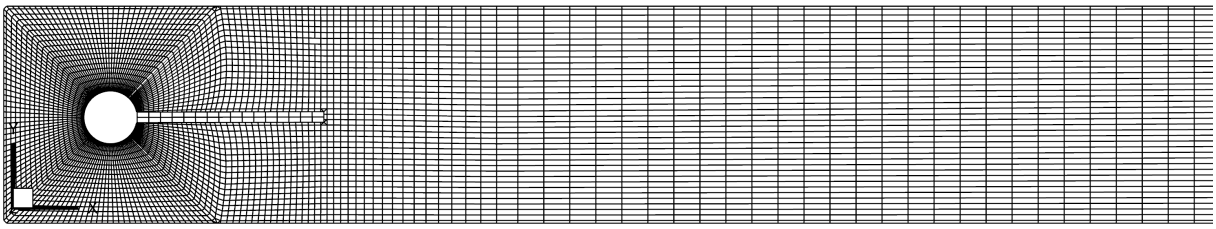

Figure 4: Non matching fluid and structure grid

The channel has the dimensions $2.5 \times 0.41 \times 0.1$ [m^3], with a slightly off symmetric positioned cylinder at $(0.2[\text{m}], 0.2[\text{m}])$, radius 0.05 [m] and a bar attached to the cylinder

of size $0.35 \times 0.02 \times 0.1$ [m^3].
The computational domain is discretized into 2,048 elements for the structure part and 80,384 volumes for the fluid. Figure 4 shows the one time coarsened nonmatching grids for the fluid and structure domain. Boundary conditions for the fluid are: Parabolic inflow profile $v_f = 1.5\ \bar{v}\left(\frac{4.0}{0.1681}\frac{y}{[\mathrm{m}]}(0.41 - \frac{y}{[\mathrm{m}]}), 0\right)^T$, with $\bar{v} = 0.2\ [\frac{\mathrm{m}}{\mathrm{s}}]$, Dirichlet outlet condition, symmetry boundary condition in z direction and no-slip on all other faces. The structure is clamped at the cylinder and fixed in z direction at $z = 0$ and $z = 0.1$[m].
The fluid field is initialized with constant velocity $v_f = (\bar{v}, 0)^T$, the structure is initially at rest without any loading.
The fluid is set to be incompressible and Newtonian with density $\rho = 1\ [10^3 \frac{\mathrm{kg}}{\mathrm{m}^3}]$ and dynamic viscosity $\mu_f = 1\ [\frac{\mathrm{kg}}{\mathrm{ms}}]$. This leads to a Reynolds number of Re $= 20$. The structure is linear elastic with Youngs modulus $E = 1.4\ [10^6 \frac{\mathrm{kg}}{\mathrm{ms}^2}]$ and Poisson ratio $\nu = 0.4$.

5.2 Results

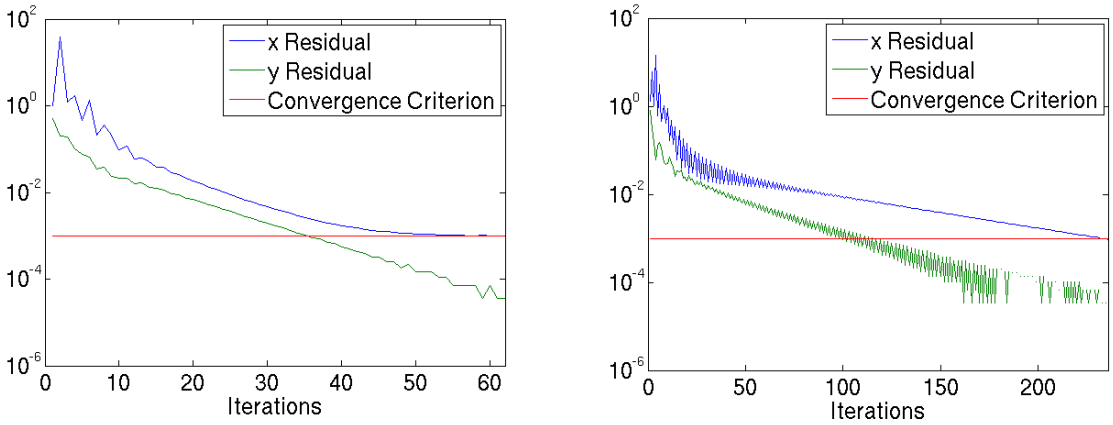

Figure 5: Course of residuals using **MG**(left) and **SG** (right)

In order to compare the two approaches, two setups are specified. First, the implicit partitioned coupling approach with global multigrid (**MG**). The flow solver FASTEST is accelerated by geometric multigrid with the SIP as linear system solver. The structure solver FEAP is accelerated by a geometric multigrid with a Gauß-Seidel linear system solver and LAPACK direct solver on the coarsest grid. Coupling is applied at every grid level.
Second, the implicit partitioned coupling approach (**SG**). The flow solver FASTEST is accelerated by geometric multigrid with the SIP as linear system solver. The structure solver FEAP uses a conjugate gradient method on a single grid. Coupling is only performed on the finest grid.
As convergence criterion the relative displacement in the current FSI iteration n is utilized: $\frac{u_n - u_{n-1}}{u_{n-1}} < 10^{-3}$. Figure 5 depicts the course of this quantity for both setups. The

Setup	# V-cycles	# Fine Grid Iterations
SG	233	2330
MG	59	1180

Table 2: Numbers of iterations until convergence

coupled computation in **MG** as well as the flow computation in **SG** are both performed on two grid levels. For **MG**, two coupling steps within every grid level have been found useful.
As the initial conditions of this test case are not at physical equilibrium, underrelaxation of the exchanged values is unavoidable. The parameters used are $\lambda_u = 1.0$ for the displacements and $\lambda_f = 0.03$ for the force. In order not to alter the results, underrelaxation is applied as $f_{\text{resulting}} = \lambda_f f_{\text{new}} + (1 - \lambda_f) f_{\text{old}}$.
Figure 6 shows the fluid velocity and structure displacement at the end of the computation. Table 2 denotes the number of V-cycles and fine grid iterations required by the flow solver for both setups. **MG** needs about one quarter of the V-cycles needed by **SG**, though the latter approach is using only half as many fine grid iterations per cycle. Thus the computational work is about half.

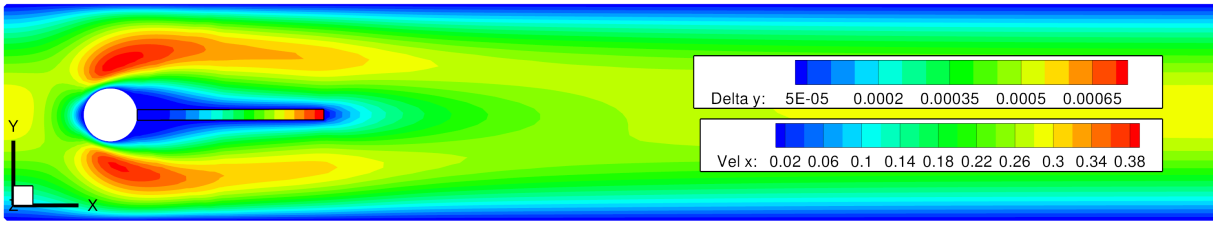

Figure 6: x Velocity and y Displacement

6 CONCLUSIONS

A global multigrid method for coupled FSI problems has been introduced. This method advances the implicit partitioned approach closer towards the monolithic approach. In contrast to the implicit partitioned coupling, errors arising from the coupling procedure are also eliminated on coarse grids, thus reducing the numbers of overall solution iterations and, finally, computing time. This is achieved by extending the multigrid method, which is an established acceleration technique in fluid solvers, to the coupled FSI system. Utilizing the full approximation scheme as nonlinear multigrid method, the coupling subroutines remain, to a large extend, unchanged. Test case I shows the linear dependence of computation cost with respect to the discretization when using the multigrid method for structure problems. Test case II shows an application of the global multigrid method to a 3D FSI problem and very promising results in comparison with single grid coupling. The

next step is to validate the linear dependence of the global multigrid FSI implementation with respect to discretization and to compare it with partitioned and monolithic solvers.

Acknowledgements

This work is supported by the 'Excellence Initiative' of the German Federal and State Governments and the Graduate School of Computational Engineering at Technische Universität Darmstadt.

REFERENCES

[1] Anderson, E. and Bai, Z. and Bischof, C. and Blackford, S. and Demmel, J. and Dongarra, J. and Du Croz, J. and Greenbaum, A. and Hammarling, S. and McKenney, A. and Sorensen, D., *LAPACK Users' Guide*, Third Edition, Society for Industrial and Applied Mathematics, 1999

[2] W. L. Briggs, *A Multigrid Tutorial*, Society for Industrial and Applied Mathematics, 2000.

[3] I. Demirdzic and M. Peric, Space Conservation Law in Finite Volume Calculations of Fluid Flow, *Int. Journal for Numerical Methods in Fluids*, Vol. 8, 1988

[4] J. Donea, *Computational Methods for Transient Analysis, Computational Methods in Mechanics*, Volume 1, chapter Arbitrary Lagrangian Eulerian Methods, Elsevier, North-Holland, 1983.

[5] H. L. Dütsch, *Numerische Simulation mechanischer Fluid-Struktur-Wechselwirkung bei grossen Auslenkungen*, PhD Thesis, Universität Erlangen-Nürnberg, 2000.

[6] T. Dunne, *Adaptive Finite Element Approximation of Fluid-Struture Interaction Based on Eulerian and Arbitrary Lagrangian-Eulerian Variational Formulations*, PhD Thesis, Ruprecht-Karls Universität Heidelberg, 2007.

[7] *FASTEST User Manual*, Fachgebiet Numerische Berechnungsverfahren im Maschinenbau, Technische Universität Darmstadt, 2005.

[8] R. L. Taylor, *FEAP - a finite element analysis program*, Version 8.2, University of California, Berkeley, 2008.

[9] W. Hackbusch, *Mulit-Grid Methods and Applications*, Springer, 1985.

[10] M. Heck, *Mehrgitterverfahren zur effizienten numerischen Simulation von Fluid-Strucktur Wechselwirkungen*, PhD-Thesis, Technische Universität Darmstadt, 2008.

[11] J. Hron, S. Turek, A Monolithic FEM/Multigrid Solver for an ALE Formulation of Fluid-Structure Interaction with Applications in Biomechanics, in *Fluid-Structure Interaction*, H.-J. Bungartz and M. Schäfer, editors. Volume 53 of *Lecture Notes in Computational Science and Engineering*.

[12] *MpCCI Mesh-based parallel code coupling interface*, User guide, Fraunhofer Institut für Algorithmen und wissenschaftliches Rechnen SCAI, Bonn, 2007.

[13] The Multigrid Method in Solid Mechanics: Part 1- Algorithm Description and Behavior, in *Int. Journal for Numerical Methods in Engineering*, Vol. 29 No. 1, 1990

[14] S. Rugonyi, K. J. Bathe, On Finite Element Analysis of Fluid Flows Fully Coupled with Structural Interactions, in *CMES*, Vol. 2 No. 2, 2001

[15] S. P. Spekreijse, Elliptic Grid Generation Based on Laplace Equations and Algebraic Transformations, *Journal of Computational Physics*, 1995.

[16] D. Sternel, M. Schäfer, M. Heck, S. Yigit, Efficiency and accuracy of fluid-structure interaction simulations using an implicit partitioned approach. *Computational Mechanics*, 2008.

[17] H. L. Stone, Iterative Solution of Implicit Approximations of Multidimensional Partial Differential Equations, in *SIAM Journal on Numerical Analysis*, Vol. 5 No. 3, 1968

[18] S. Turek, J. Hron, Proposal for Numerical Benchmarking of Fluid-Structure Interaction between an Elastic Object and Laminar Incompressible Flow, in *Fluid-Structure Interaction*, H.-J. Bungartz and M. Schäfer, editors. Volume 53 of *Lecture Notes in Computational Science and Engineering*.

[19] S. Yigit, Efficiency of Fluid-Structure Interaction Simulations with Adaptive Underrelaxation and Multigrid Acceleration, in *Int. Jnl. of Multiphysics*, Vol. 1 No. 1, 2007.